



ESA/Contract No. 4000126561/19/I-NB

Consortium Members



ESA Sea Level CCI+

# Noise and climate variability impact on coastal trends uncertainties

Nomenclature: SLCCI+\_TN\_058\_NoiseClimVar\_Uncertainties

Issue: 1.0

Date: Jan. 11, 23





Chronology Issues:			
Issue:	Date:	Reason for change:	Author
1.0	11/01/23	Initial Version	J. Oelsmann (TUM)

People involved in this issue:		
Written by:	J. Oelsmann (TUM)	
Checked by:	JF Legeais (CLS)	
Approved by:	JF Legeais (CLS)	

Acceptance of this deliverable document:			
Accepted by ESA:	J. Benveniste (ESA)	<date>	<Signature>

Distribution:		
Company	Names	Contact Details
ESA	J. Benveniste A. Ambrozio, M. Restano	<a href="mailto:Jerome.Benveniste@esa.int">Jerome.Benveniste@esa.int</a> ; <a href="mailto:Americo.Ambrozio@esa.int">Americo.Ambrozio@esa.int</a> ; <a href="mailto:Marco.Restano@esa.int">Marco.Restano@esa.int</a>
CLS	J.-F. Legeais ; P. Prandi ; S. Labroue	<a href="mailto:jlegeais@groupcls.com">jlegeais@groupcls.com</a> ; <a href="mailto:pprandi@groupcls.com">pprandi@groupcls.com</a> ; <a href="mailto:slabroue@groupcls.com">slabroue@groupcls.com</a> ;
LEGOS	A. Cazenave ; B. Meyssignac ; F. Birol; F. Nino; F. Leger;	<a href="mailto:anny.cazenave@legos.obs-mip.fr">anny.cazenave@legos.obs-mip.fr</a> ; <a href="mailto:Benoit.Meyssignac@legos.obs-mip.fr">Benoit.Meyssignac@legos.obs-mip.fr</a> ; <a href="mailto:florence.birol@legos.obs-mip.fr">florence.birol@legos.obs-mip.fr</a> ; <a href="mailto:fernando.nino@legos.obs-mip.fr">fernando.nino@legos.obs-mip.fr</a> ; <a href="mailto:fabien.leger@legos.obs-mip.fr">fabien.leger@legos.obs-mip.fr</a> ;
NOC	F. Calafat	<a href="mailto:Francisco.calafat@noc.ac.uk">Francisco.calafat@noc.ac.uk</a> ;
SkyMAT Ltd	A. Shaw	<a href="mailto:agps@skymat.co.uk">agps@skymat.co.uk</a> ;
DGFI-TUM	M. Passaro J. Oelsmann	<a href="mailto:marcello.passaro@tum.de">marcello.passaro@tum.de</a> <a href="mailto:julius.oelsmann@tum.de">julius.oelsmann@tum.de</a>



List of Contents

<b>1. Introduction .....</b>	<b>4</b>
<b>2. Objectives .....</b>	<b>7</b>
<b>3. Description of tasks .....</b>	<b>7</b>
<b>3.1. Task 1: Preparation of data and methods.....</b>	<b>7</b>
<b>3.2. Task 2: Spectral analysis, trend and uncertainty computation.....</b>	<b>8</b>
<b>3.3. Task 3: Impact of climate variability on trend and trend uncertainty estimates .....</b>	<b>8</b>
<b>3.4. Task 4: Re-assessing differences between coastal and offshore trends ..</b>	<b>9</b>
<b>4. References .....</b>	<b>10</b>



## 1. Introduction

Climate-induced absolute sea level change represents a substantial threat to coastal communities, infrastructure and habitability. Global mean rates of contemporary sea level change (1995-2018, 3.1 mm/year as reported by Cazenave et al., 2018) have already doubled compared to average rate over the last century (of approximately 1.4 mm/year (Frederikse et al., 2020)) and are expected to further accelerate in the upcoming decades (Fox-Kemper et al., 2021). Hence, understanding the evolution and the causes of sea level changes is fundamental to estimate future impacts and risks along the global coastlines.

The advent of satellite altimetry almost 30 years ago has revolutionized sea level science as it has enabled global-scale observations of sea level variability and trends. Recent developments, e.g., in coastal retracking and geophysical corrections, have further improved the retrieval of valid sea level data within the first 20 km to the coast (Passaro et al., 2014, Cazenave et al., 2022), which is challenging due to the contamination of the reflected signal in the vicinity of the coast. These coastal sea level observations are crucial, because coastal sea level dynamics can be substantially different from the open ocean (Hughes et al., 2019). The presence of the continental slope, shallow waters and the lateral boundaries (i.e. the coastlines), give rise to a variety of processes which are associated with multifaceted spatio/temporal sea level characteristics (Calafat et al., 2018, Hughes et al., 2018, Hughes et al., 2019).

Understanding the sources and characteristics of sea level changes in the coastal zone is highly relevant - not only from a scientific, but even more from a socioeconomic perspective. Hence the question of 'how coastal sea level variability and trends differ from the open ocean' has become a central subject of ongoing investigations (see Vignudelli et al., 2019, Cazenave et al., 2022 or Woodworth et al., 2019, for a review). Thanks to advancements in coastal sea level products (within the previous phase of the Climate Change Initiative (CCI) Sea Level Project by the European Space Agency (ESA)), Cazenave et al., 2022 were able to systematically assess to what extent coastal sea level trends differ from offshore sea level trends ('offshore' was here defined as averages within a 15-17km distance). They found significant differences at 22% of the virtual stations, i.e. coastal intersects of the altimetry track. Several potential physical sources of these differences, such as coastal currents, wind and waves, or river runoff, as well as potential processing errors were discussed (Cazenave et al., 2022; Gouzenes et al., 2020). However, they did not come to general conclusions of the causes of these differences, mainly due to the lack of data or models at the sites and at such high resolutions.

One central aspect for the determination of coastal sea level trends in the coastal zone and their discrepancies with respect to offshore trends is the treatment of trend uncertainties, which are finally used to define the significance of these trend differences. Cazenave et al., 2022 computed uncertainties from the 1-sigma standard-errors of a standard least-squares fit of the sea level anomaly time series (assuming white noise), noting that more advanced uncertainty analyses might be required. Previous research has highlighted that taking into account serial correlation and the spectral properties of the residuals is indeed crucial to accurately determine uncertainties in the parameters such as trends (Williams, 2003; Bos et al., 2013; Royston et al., 2018). Not accounting for autocorrelation in the data, or applying inadequate models to estimate correlated noise can lead to an underestimation of uncertainties up to one order of magnitude (Bos et al., 2013).

However, currently we have only limited knowledge of the spectral properties of sea level variability in the coastal zone, and how these properties change, e.g., depending on the distance to coast, water depth, latitude or shelf width. To our knowledge, there exist no study which has yet systematically estimated these properties using coastal altimetry products on a global scale. Existing studies are currently confined to either global tide gauge datasets (Bos et al., 2014) or altimetry data for selected regions (Royston et al., 2018). Hence, applying a more rigorous uncertainty quantification is crucial, not only to better understand the temporal characteristics of coastal sea level dynamics, but also to re-assess previous work (Cazenave et al., 2022) to shed light on the statistical significance of differences between coastal and open ocean sea level trends.

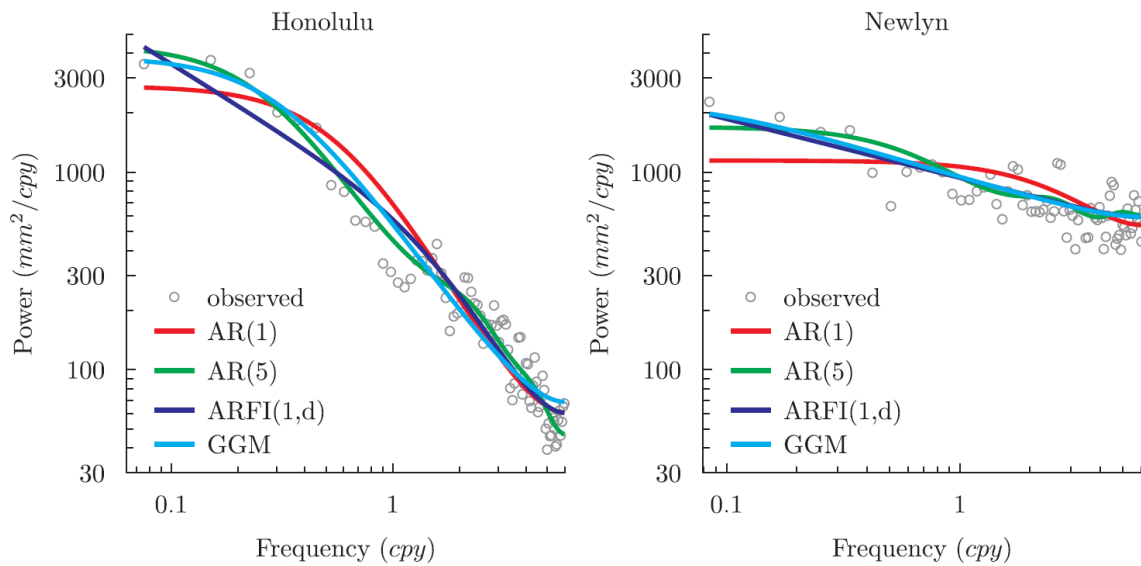


Figure 1: Power spectral density plots for the sea level residuals at Honolulu and Newlyn tide gauges (from Bos et al., 2014)

Serial correlation in sea level anomaly time series is caused by a superposition of processes which are associated with different time-scales of persistence ranging from annual, interannual to decadal periods. To account for serial correlation of the residual time series previous studies applied different models, e.g., such as a first order autoregressive AR(1) model (Benveniste et al., 2020, Nerem et al., 2010). Viewed in a power spectral density plot, the power of AR(1) noise flattens at low frequencies compared to higher order models, e.g., AR(5) or auto-regressive fractionally-integrated moving-average (ARFIMA, ARFI, or later called power-law) models (as shown in Figure 1, from Bos et al., 2014). The latter models have been shown to describe the power spectral features of sea level anomalies more realistically in the majority of cases (Hughes & Williams, 2010, Bos et al., 2014, Royston et al., 2018). The power law model (ARFI) determines the relationship between power and frequency as a function of the spectral index  $k$  (or sometimes expressed as  $k = 2d$ ), such that spectral power is increasing at low frequencies:

$$P(f) = P_0 \left( \frac{f}{f_0} \right)^k$$

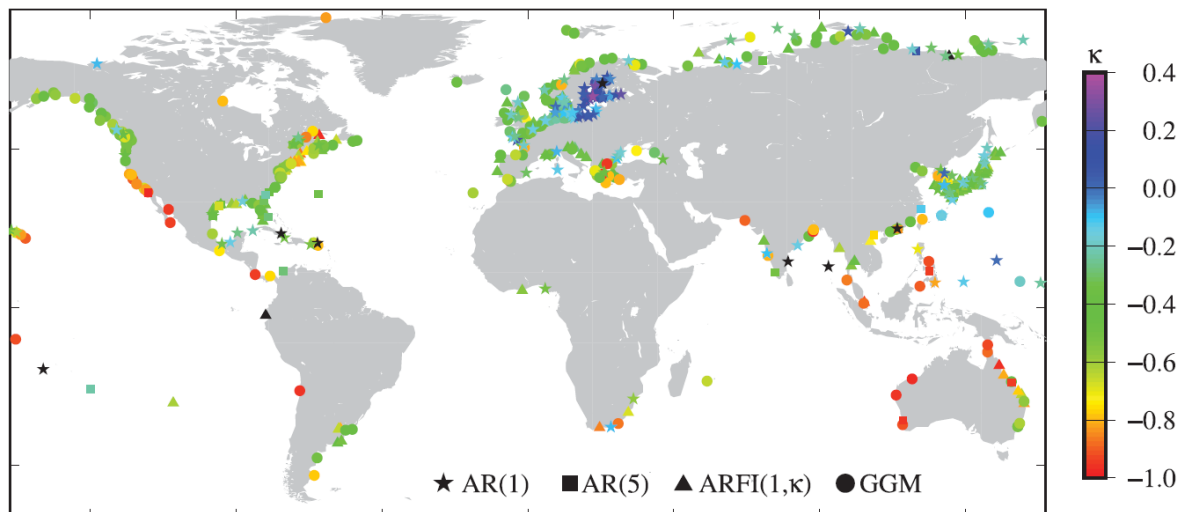


Figure 2: The estimated value of  $\kappa$  using the ARFI(1,  $\kappa$ ) model. The shape of the symbol represents which stochastic model has the lowest BIC values (from Bos et al., 2014).

The dependency of trend uncertainties on the properties and choice of the noise model was made clear by Bos et al., 2014 in Figure 1. Here, different noise models (AR(1), AR(5) and GGM (Generalized Gauss Markov)) were applied for tide gauge data from the site at Honolulu, resulting in different trend uncertainties of 0.12, 0.15 and 0.14 mm/y, respectively. In contrast, the power-law model



(ARFI(1,  $k$ )), which does not flatten out at low frequencies resulted in much a larger uncertainty of 0.33 mm/y. To choose the best-fitting model, commonly the statistics Akaike Information Criteria (AIC; Akaike, 1973) and Bayesian Information Criteria (BIC; Schwarz, 1978) are analysed (e.g., Royston et al., 2018). These statistics give a measure of model complexity and model fit, and hence penalize overly complex models (even in case they have a very good model fit). The model with the lowest AIC or BIC criteria is usually selected as the preferred one (Bos et al., 2016). As an example, In the case of Honolulu, the GGM model has the best fit according to the BIC criterion. As shown by the differences of the spectral properties of the site at Honolulu and Newlyn, a regional analysis is required to identify the most appropriate model depending on the site/region. Such regional dependencies are also depicted in Figure 2, where different noise models were applied to tide gauge data. The spectral properties strongly depend on the region as shown by the spectral index and the type of the best-fitting noise model.

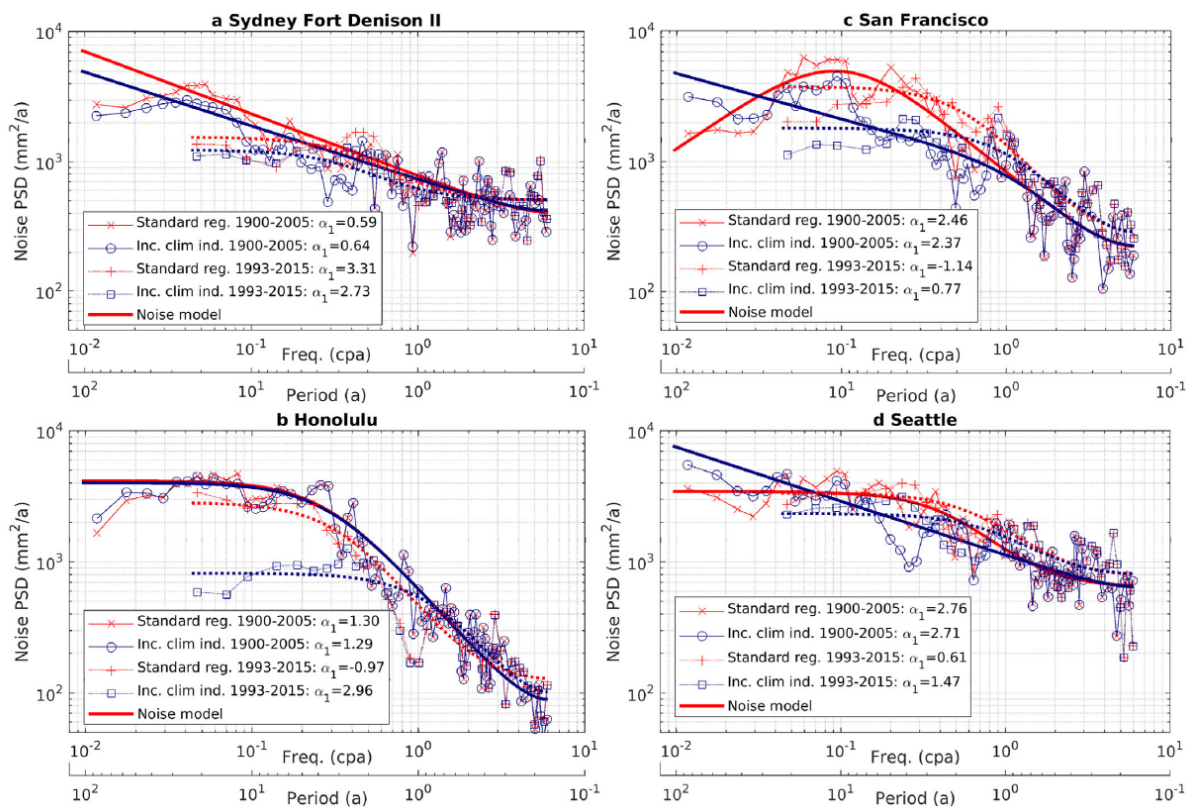


Figure 3: Power spectral density plots of noise for four long-duration tide gauge time series, with (blue) and without (red) climate indices included in the regression: (a) Sydney Fort Denison II, (b) Honolulu, (c) San Francisco and (d) Seattle.  $\alpha_1$  is the trend coefficient estimate (from Royston et al., 2018). Dotted lines show noise model fits for a shorter period of time (1993-2015), with respect to the full time period (1900-2005, solid lines).

One important contributor of low-frequency noise are climate modes (e.g., such as ENSO, PDO or NAO), which have been shown to explain significant fractions of sea level variability at regional scales (Royston et al., 2018, Wang et al., 2020). Due to the relative shortness of current altimetry-based records (i.e. ~30 years) these modes can also influence trends themselves, when they are estimated over the altimetry era (Passaro et al., 2021), and can have a significant impact on trend uncertainties and thus also the time of emergence (ToE, Royston et al., 2018). As an example, Figure 3 shows the power spectral density plots for the noise from four long duration tide gauge time series from Royston et al., 2018. These examples show fits of different noise models depending on time series length and depending on whether climate indices were included in the regression analysis or not. As can be seen, the spectral properties, as well as the magnitudes of the estimated trends can change, depending on whether these climate indices are explicitly included, or not. However, the influence of climate modes on coastal sea level variability has so far not been systematically quantified based on a comprehensive database of coastal altimetry products. It is currently unclear how their influence will affect trends and trend uncertainties in the coastal zone.



## 2. Objectives

In summary, there is limited knowledge of spectral properties of coastal sea level variations and how they differ compared to the open ocean variations, as previous analyses did not yet tackle these issue using global-scale coastal altimetry data. Here we aim to overcome these limitations by answering the following research questions:

- How does low-frequency noise influence the formal uncertainties of sea level trends in the coastal zone?
- What is the time scale of emergence of coastal and open ocean sea level trends, and how do coastal and open ocean trends differ from each other?
- What fraction of trends and uncertainties are explained by climate modes and how do climate modes affect trends and uncertainties?

Our investigations are organised into four different tasks. First (1) we will prepare the datasets including coastal altimetry data, climate indices, tide gauges, and other auxiliary products and set-up the software to efficiently perform spectral analyses. Secondly (2) we will perform the spectral analysis, as well as the trend and uncertainty computation. This step will be repeated (3) under the consideration of climate variability in the regression model. Finally (4), we will re-assess differences between coastal and open ocean trends, depending on the updated uncertainties and trends, and considering the impact of climate variability.

## 3. Description of tasks

### 3.1. Task 1: Preparation of data and methods

In this work package, we will prepare the coastal altimetry data and set up the model to perform the spectral analysis and trend computation. We will use the 20Hz along-track sea level anomalies (SLAs) from the XTRACK-ALES product (version v2.2: <https://doi.org/10.17882/74354>). This data set is based on the missions Jason 1,2 and 3 missions and covers the period from January 2002 to December 2019. The data will be re-sampled to monthly averages and we will re-compute virtual stations (as intersects of the along-track data with the coastline). We will investigate different criteria of defining data as 'coastal' or 'open ocean'. These criteria will be based on the distance to coast, correlation-length scale and water depth. The correlation length-scale  $\lambda$  will be derived by fitting an exponential decay function  $corr(d) = scale * e^{-d/\lambda}$  to the correlations of SLA along a track (computed with respect to the average within 0-5 km to the coast) sorted by distance to coast  $d$ . We suggest to apply the following selection criteria:

Selection	$d$	$\lambda$	depth
Coastal	0-5 km	$0 \leq x < \lambda$	0-200m
	0-10 km	$0 \leq x < \lambda/2$	0-1000m
	Closest point to coast		
Open ocean	15-17 km,	$2\lambda > x > \lambda$	1500-3000m
	100-200 km	$3\lambda > x > 1.5\lambda$	3000-4000m
	200-300 km		

We anticipate that this systematic analysis will help to find a more objective decision of what should be defined as 'coastal', or 'open ocean'. Particularly the analysis of correlation length scales will support the interpretation of the cross-shelf coherency of SLAs.

Next to the altimetry data we will use monthly PSMSL tide gauges (TGs, Holgate et al., 2006) for comparison. TG data will be useful to study the importance of time series length for spectral analyses



and to determine differences w.r.t. altimetry data. We will also include climate indices, which will be taken from different data providers, i.e., they will not be explicitly derived from SST or SLP anomalies. Finally, we will integrate the Hector Software (Bos et al., 2016) in a Python framework, such that it can be run in parallel to enable efficient analysis of the data. Hector is based on maximum likelihood estimation and is capable to estimate different parameters (i.e., trend, offset, annual cycle, noise parameters) of a combination of deterministic and stochastic models.

### 3.2. Task 2: Spectral analysis, trend and uncertainty computation

In this task we will perform a spectral analysis of the altimetry and tide gauge time series. We will investigate which noise model most adequately fits the spectral properties. For this purpose, we will test different noise models: White noise (WN), power law plus white noise (PLWN), AR(1) plus white and a Generalized Gauss Markov (GGM) plus white noise model (more detailed descriptions on the noise model formulations and associated covariance matrices can be found in Langbein, 2004, Bos et al., 2008, and Williams et al., 2008). At every location, we fit the sea level time series to estimate offset  $a_0$ , trend  $a_1$ , the annual and semi-annual cycle ( $a_2, a_3, \phi_a, \phi_{sa}$ ) as well as parameters of the noise model:

$$SL_t = a_0 + a_1 t + a_2 \cos(2\pi t + \phi_a) + a_3 \cos(4\pi t + \phi_{sa}) + \epsilon$$

The best noise model will be selected according to the AIC and BIC statistics, as done in Bos et al., 2014 or Royston et al., 2018. We will particularly focus on the spectral index  $k$  estimated in the PLWN model, which defines the dependency of the power of the noise on frequency  $P(f) = P_0(f/f_0)^k$ . This parameter is important for the interpretation of trend uncertainties, which are particularly increased by low-frequency noise. As can be seen in Figure 4, for different  $k$ , we obtain different noise properties: White noise for  $k = 0$ , Flicker noise  $k = -1$  for and random walk noise for  $k = -2$ .

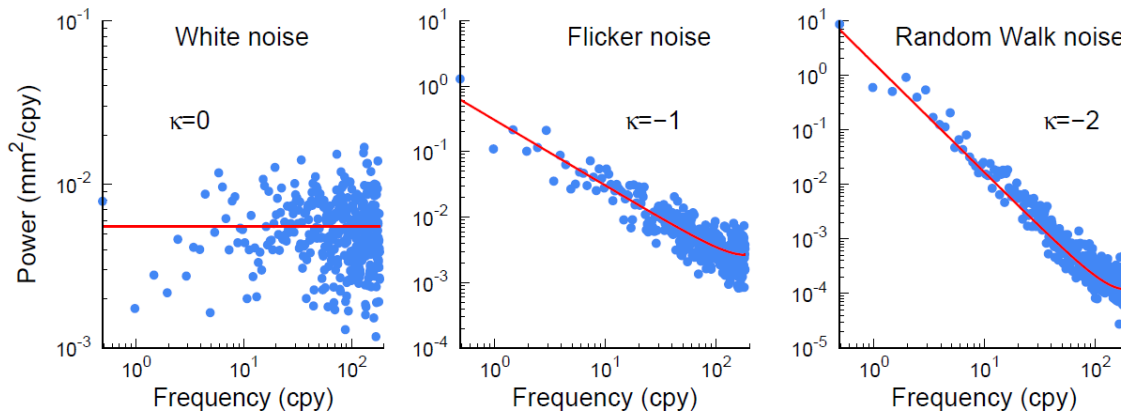


Figure 4: One-sided power spectral density for white, flicker and random walk noise. The blue dots are the computed periodogram (Welch's method) while the solid red line is the fitted power-law model (from Bos et al., 2019).

All parameters will be estimated for the different time series (SAT and TG), derived in Task 1 as well as the different selection criteria. This dataset will be the first deliverable D1.

### 3.3. Task 3: Impact of climate variability on trend and trend uncertainty estimates

In this task we will repeat the analyses performed in Task 2 by incorporating climate index time series  $CI_c$  in the multivariate regression model as follows:

$$SL_t = a_0 + a_1 t + a_2 \cos(2\pi t + \phi_a) + a_3 \cos(4\pi t + \phi_{sa}) + \sum_{c=0}^n a_{4+c} CI_c + \epsilon$$

We will incorporate eight different indices, namely the NAO, EA, PNA, EA, SCA, AO, ENSO and PDO. With this analysis we seek to understand how much variance of coastal sea level variability is explained by which climate mode, how trends and trend uncertainties are influenced by these modes,



and at what frequencies the modes have the largest impact. This analysis will also improve our understanding of the causes of interannual to decadal sea level changes along the coastlines. The outcome of this Task will be the deliverable D2 and is an analogue to the data provided in D1.

### 3.4. Task 4: Re-assessing differences between coastal and offshore trends

Based on D1 and D2, we will re-assess differences between coastal and open ocean variability and trends. Before we can do so, we will first investigate an appropriate approach to select ‘coastal’ and ‘open ocean’ sea level data. We will consider different parameters to evaluate differences between different selection criteria of coastal and open ocean data: Trends, trend uncertainties, spectral index, driving-noise (the noise that scales the amplitude of the noise models) and standard-deviation.

In a second step we will re-assess the significance of the differences between coastal and open ocean trends. We will compute the significance ratio  $SE = (t_{coast} - t_{openocean}) / \sqrt{\sigma_{coast}^2 + \sigma_{openocean}^2}$ , i.e. the ratio of trend differences over the combined error. If  $|SE| > 1$  trend differences will be defined as significant (when the 95% CI trend uncertainties are considered). This analysis will be repeated for different coastal SL time series selections (as described before) and discussed in light of other parameters (depth, distance to coast, correlation length scale, latitude).

Finally, we will compute the time of emergence (ToE) of the coastal and open ocean sea level trends, as well as the time scale at which coastal and open ocean sea level trends become not significant from each other anymore, hereinafter called time of agreement (ToA). To compute the ToE we will investigate two different approaches. The first approach was put forward by Royston et al., 2018, who defined the ToE as the time scale at which a trend (of arbitrary magnitude) exceeds the noise level of a time series at a particular location. To define this time scale, we will simulate 1,000 surrogate stochastic noise time series of sufficient length (e.g., 100 years) based on the same noise properties as estimated at a particular location. Next, based on the 1,000 samples we will generate a distribution of time scales at which a given trend (varied in the range from 0.5-10 mm/y) exceeds the simulated noise, as illustrated in Figure 5. A spline function will be applied to fit the dependency between ToE and magnitude of trend. This function will be used to determine the ToE for an observed trend at every individual location.

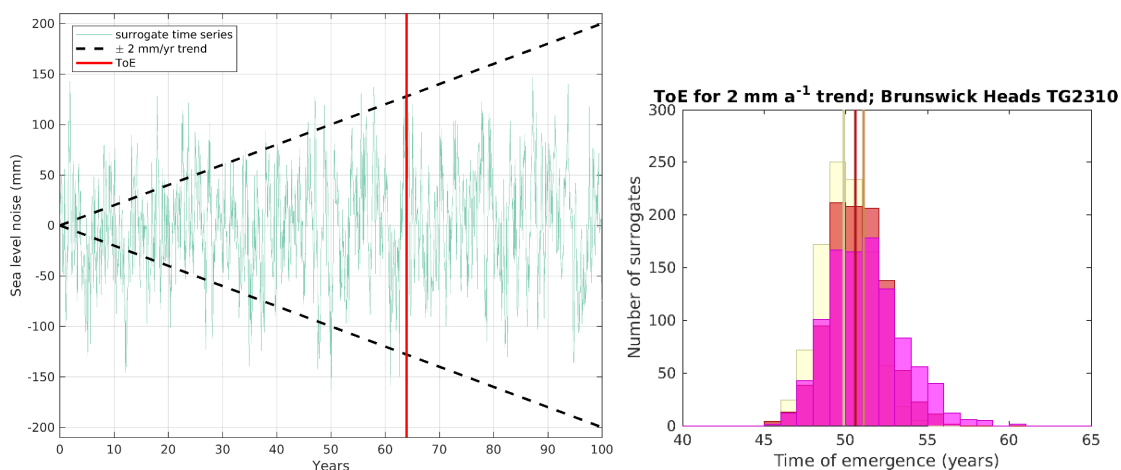


**Figure 5:** Figure S1 and S2 modified from the supporting information file from Royston et al., 2018. Figure S1(left): Methodology for the Time of Emergence (ToE; a) calculation: One example surrogate noise time series, with the ToE for a  $\pm 2 \text{ mm a}^{-1}$  trend to emerge from this instance. The ToE is calculated for all 1,000 surrogate time series giving the distribution of ToE for each location; examples of the different ToE distributions obtained with different noise models are given in Figure S2. Figure S2 (right): Example histograms of the time of emergence (ToE; a) from 1,000 sample surrogate noise time series, assuming white noise, AR(1) noise and the most appropriate noise model, for a given trend of  $2 \text{ mm a}^{-1}$ : (only a is shown here) Brunswick Heads, Australia. The data comprises the epoch 1993–2015 and the most appropriate noise model in both data sets is power-law.



As an alternative approach we will define the ToE as the time scale at which a given trend exceeds the trend uncertainty for a given period of time. For this purpose, we will determine an empirical function of the dependency of trend uncertainty on time scale at any given location and noise. This dependency will be computed by estimating trend uncertainties based on a 10-member-ensemble of synthetically generated noise time series with varying period lengths (i.e., with 5,10,15 years, ...).

This relationship between trend uncertainty and time scale will be exploited to compute the ToA, i.e. the time scale when coastal and open ocean trends are not significant from each other anymore ( $ToA|_{|SE| \leq 1}$ ). In addition, we will also compute the ToA between a local (i.e., coastal sea level) trend and the GMSL trend. The outcome of this task will be a dataset (deliverable D3) containing the ToE, ToA, as well as the SE at different coastal-open ocean pairs.

## 4. References

- Akaike, H. (1973). Information theory and an extension of the maximum likelihood principle. In B. N. Petrov and S. Caski (Eds.), Proceedings of the second international symposium on information theory (pp. 267-281). Budapest: Akademiai Kiado.
- Benveniste, J. et al. Coastal sea level anomalies and associated trends from Jason satellite altimetry over 2002-2018. *Nat. Sci. Data* 7, 357 (2020).
- Bos, M.S., Fernandes, R.M.S., Williams, S.D.P. et al. Fast error analysis of continuous GNSS observations with missing data. *J Geod* 87, 351-360 (2013). <https://doi.org/10.1007/s00190-012-0605-0>
- Bos MS, Fernandes RMS, Williams SDP, Bastos L (2008) Fast error analysis of continuous GPS observations. *J Geod* 82:157-166. doi:10.1007/s00190-007-0165-x
- Bos, M. S., Williams, S. D. P., Araújo, I. B., Bastos, L. The effect of temporal correlated noise on the sea level rate and acceleration uncertainty, *Geophysical Journal International*, Volume 196, Issue 3, March 2014, Pages 1423-1430, <https://doi.org/10.1093/gji/ggt481>
- Bos, M., & Fernandes, R. (2016). Hector user manual version 1.6 (Tech. Rep.). Covilh-a, Portugal: SEGAL Universidade da Beira Interior.
- Bos, M. S., Montillet, J.-P., Williams, S. D. P., and Fernandes, R. M. S. (2019). Introduction to geodetic time series analysis. *Springer Geophysics*, page 29–52.
- Calafat, F. M., Wahl, T., Lindsten, F., Williams, J., and Frajka-Williams, E.: Coherent modulation of the sea-level annual cycle in the United States by Atlantic Rossby waves, *Nat. Commun.*, 9, 2571, <https://doi.org/10.1038/s41467-018-04898-y>, 2018.
- Cazenave A., Y. Gouzenes, F. Birol, F. Leger, M. Passaro, F. M. Calafat, A. Shaw, F. Nino, J.-F. Legeais, J. Oelmann, M. Restano and J. Benveniste, Sea level along the world's coastlines can be measured by a network of virtual altimetry stations. *Commun Earth Environ* 3, 117 (2022). <https://doi.org/10.1038/s43247-022-00448-z>
- Frederikse, T., Landerer, F., Caron, L., Adhikari, S., Parkes, D., Humphrey, V. W., Dangendorf, S., Hogarth, P., Zanna, L., Cheng, L., and Wu, Y.-H. (2020). The causes of sea-level rise since 1900. *Nature*, 584(7821):393-397.
- Gouzenes, Y. et al. Coastal sea level change at Senetosa (Corsica) during the Jason altimetry missions. *Ocean Sci.* 16, 1-18 (2020).
- Hughes, C. W., & Williams, S. D. P. (2010). The color of sea level: Importance of spatial variations in spectral shape for assessing the significance of trends. *Journal of Geophysical Research*, 115, C10048. <https://doi.org/10.1029/2010JC006102>
- Hughes, C.W., Joanne Williams, J., Blaker, A., Coward, A., Stepanov, V., A window on the deep ocean: The special value of ocean bottom pressure for monitoring the large-scale, deep-ocean circulation, *Progress in Oceanography*, Volume 161, 2018, Pages 19-46, ISSN 0079-6611, <https://doi.org/10.1016/j.pocean.2018.01.011>.



Hughes, C. W., Fukumori, I., Griffies, S. M., and Huthnance, J. M.: Sea Level and the Role of Coastal Trapped Waves in Mediating the Influence of the Open Ocean on the Coast, *Surv. Geophys.*, 40, 1467-1492, <https://doi.org/10.1007/s10712-019-09535-x>, 2019.

Langbein J (2004) Noise in two-color electronic distance meter measurements revisited. *J Geophys Res* 109(B04406). doi:10.1029/2003JB002819

Nerem, R.S., Chambers, D., Choe, C. & Mitchum, G.T., 2010. Estimating mean sea level change from the TOPEX and Jason Altimeter missions, *Mar. Geod.*, 33(1), 435-446.

Oelsmann, J., Passaro, M., Dettmering, D., Schwatke, C., Sánchez, L., and Seitz, F. (2021). The zone of influence: matching sea level variability from coastal altimetry and tide gauges for vertical land motion estimation. *Ocean Science*, 17(1):35-57.

Passaro, M., Cipollini, P., Vignudelli, S., Quartly, G. D., and Snaith, H. M.: ALES: A multi-mission adaptive subwaveform retracker for coastal and open ocean altimetry, *Remote Sens. Environ.*, 145, 173-189, <https://doi.org/10.1016/j.rse.2014.02.008>, 2014.

Passaro M, Müller FL, Oelsmann J, Rautiainen L, Dettmering D, Hart-Davis MG, Abulaitijiang A, Andersen OB, Høyer JL, Madsen KS, Ringgaard IM, Särkkä J, Scarrott R, Schwatke C, Seitz F, Tuomi L, Restano M and Benveniste J (2021) Absolute Baltic Sea Level Trends in the Satellite Altimetry Era: A Revisit. *Front. Mar. Sci.* 8:647607. doi: 10.3389/fmars.2021.647607

Royston, S., Watson, C. S., Leger, B., King, M. A., Church, J. A., & Bos, M. S. (2018). Sea-level trend uncertainty with Pacific climatic variability and temporally-correlated noise. *Journal of Geophysical Research: Oceans*, 123, 1978-1993. <https://doi.org/10.1002/2017JC013655>

Vignudelli, S. et al., Satellite altimetry measurements of sea level in the coastal zone. *Surveys Geophys.* <https://doi.org/10.1007/s10712-019-09569-1>, 2019.

Wang, J., Church, J. A., Zhang, X., and Chen, X. (2021). Reconciling global mean and regional sea level change in projections and observations. *Nat Commun*, 12(1):990.

Williams, S. The effect of coloured noise on the uncertainties of rates estimated from geodetic time series. *Journal of Geodesy* 76, 483-494 (2003). <https://doi.org/10.1007/s00190-002-0283-4>

Williams SDP (2008) CATS: GPS coordinate time series analysis software. *GPS Solutions* 12(2):147-153. doi:10.1007/s10291-007-0086-4

Woodworth, P. L., Melet, A., Marcos, M., Ray, R. D., Wöppelmann, G., Sasaki, Y. N., Cirano, M., Hibbert, A., Huthnance, J. M., Monserrat, S., and Merrield, M. A. (2019). Forcing factors affecting sea level changes at the coast. *Surveys in Geophysics*, 40(6):1351-1397.

Schwarz, G. (1978). Estimating the dimension of a model. *The Annals of Statistics*, 6(2), 461-464.



End of the document